Ground state of rotating ultracold quantum gases with anisotropic spin–orbit coupling and concentrically coupled annular potential*

Wang Xin(王 鑫)[a)b)], Tan Ren-Bing(谭仁兵)[c)], Du Zhi-Jing(杜志静)[a)], Zhao Wen-Yu(赵文宇)[a)b)], Zhang Xiao-Fei(张晓斐)[a)†], and Zhang Shou-Gang(张首刚)[a)]

[a)] *Key Laboratory of Time and Frequency Primary Standards, National Time Service Center, Chinese Academy of Sciences, Xi'an* 710600, *China*
[b)] *University of Chinese Academy of Sciences, Beijing* 100049, *China*
[c)] *Department of Physics, School of Mathematics and Physics, Chongqing University of Science and Technology, Chongqing* 401331, *China*

(Received 16 December 2013; revised manuscript received 11 January 2014; published online 22 May 2014)

Motivated by recent experimental realization of synthetic spin–orbit coupling in neutral quantum gases, we consider the quasi-two-dimensional rotating two-component Bose–Einstein condensates with anisotropic Rashba spin–orbit coupling subject to concentrically coupled annular potential. For experimentally feasible parameters, the rotating condensate exhibits a variety of rich ground state structures by varying the strengths of the spin–orbit coupling and rotational frequency. Moreover, the phase transitions between different ground state phases induced by the anisotropic spin–orbit coupling are obviously different from the isotropic one.

Keywords: Bose–Einstein condensate, spin–orbit coupling, quantum phase transition

PACS: 03.75.Mn, 05.30.Jp, 67.85.Fg **DOI:** 10.1088/1674-1056/23/7/070308

1. Introduction

Spin–orbit coupling (SOC), the interaction between the spin and the momentum of a quantum particle, plays a crucial role in many important condensed matter phenomena and applications, such as anomalous and spin Hall effects, topological insulator, spintronic devices, etc.[1–4] The recent experimental breakthrough on the realization of SOC for ultracold quantum gases provides us with a completely new platform for exploring SOC physics in Bose–Einstein condensates (BEC).[5–10] A major merit of such a system lies in the unprecedented level of experimental control of the system's parameters, which thus stimulates a corresponding wave of activity focused on their ground states and collective excitations.[11–13]

So far, most of the theoretical studies on SO coupled BEC have been restricted to a free space or harmonic potential, with or without rotation.[14–33] In a recent work, the ground state properties and phase transition of a SO coupled Bose–Einstein condensate confined in concentrically coupled annular traps were investigated in detail, where various phase transitions can be induced by varying the strength of SOC.[34] Later, the combined effects of SO coupling and rotating are investigated for both pseudo spin-1/2 and spin-1 Bose gas in the same external potential by the same authors.[35,36] Nevertheless, so far only a few papers have studied the effect of anisotropic SOC on the ground state properties for a boson condensate, especially for the system confined in concentrically coupled annular potential.

Based on the studies mentioned above, the present paper reports the results of a detailed numerical analysis of the combined effects of anisotropic spin–orbit coupling and rotation on the ground state structures of a Bose–Einstein condensate confined in concentrically coupled annular potential. Based on the mean-field Gross–Pitaevskii (GP) equation, the ground state solutions are obtained by minimizing the GP energy function of the system under study. Our results show that, the introduction of anisotropic SOC leads to more rich ground state structures as compared with the case of isotropic SOC, and a number of interesting phenomena have been predicted to occur in the present system under study.

The rest of the paper is organized in the following way. We first formulate our theoretical model in Section 2, in which we also obtain the GP energy function for a Bose–Einstein condensate with anisotropic SO coupling and rotation confined in concentrically coupled annular potential. In Section 3, we investigate the ground state properties of the system as a function of the anisotropic spin–orbit coupling, and of the frequency of rotation. Finally, in Section 4, the main results of the paper are summarized.

2. Theoretical model

Our starting point is a two-component BEC with Rashba SO coupling subject to a rotation along the z direction. Within the framework of zero-temperature mean-field theory, where the collisions between the condensate atoms and the thermal cloud are neglected, and viewed from the frame of reference

*Project supported by the National Natural Science Foundation of China (Grant Nos. 11104064, 11303030, and 11174282), the National Science Fund for Distinguished Young Scholars of China (Grant No. 61025023), the National Major Fund of Scientific Equipment and Instrument Development, China (Grant No. 61127901), the Key Project Fund of the Chinese Academy of Sciences for the "Western Light" Talent Cultivation Plan, and the Science and Technology Project of Shaanxi Province, China (Grant No. 2013KJXX-03).

†Corresponding author. E-mail: xfzhang@ntsc.ac.cn

© 2014 Chinese Physical Society and IOP Publishing Ltd

corotating with the trap potential, the Hamiltonian of such a system can be written as[35]

$$\hat{H} = \hat{H}_0 + \hat{H}_{\rm int} + \hat{H}_{\rm r} + \hat{H}_{\rm so}, \tag{1}$$

where the single-particle Hamiltonian

$$\hat{H}_0 = \int {\rm d}x{\rm d}y\hat{\psi}^\dagger[-\hbar^2\nabla^2/(2m) + V_{\rm ext}(x,y)]\hat{\psi},$$

with $\hat{\psi} = [\hat{\psi}_\uparrow(\boldsymbol{r}), \hat{\psi}_\downarrow(\boldsymbol{r})]^{\rm T}$ denotes collectively the spinor Bose field operators, and m is the atomic mass (the same for both components). The interaction Hamiltonian $\hat{H}_{\rm int} = \int {\rm d}x{\rm d}y[g_{11}\hat{n}_\uparrow^2 + g_{22}\hat{n}_\downarrow^2 + 2g_{12}\hat{n}_\uparrow\hat{n}_\downarrow]$, where g_{ii} and g_{ij} account, respectively, for intra- and inter-component interactions. Without loss of generality, we assume that all the interactions are repulsive and further set $g_{11} = g_{22} = g > 0$. The rotating Hamiltonian $\hat{H}_{\rm r} = \int {\rm d}x{\rm d}y\hat{\psi}^\dagger[-\Omega\cdot\hat{L}]\hat{\psi}$ with Ω being the rotational frequency and $\hat{L}$ the angular momentum operator. The Rashba SOC Hamiltonian $\hat{H}_{\rm so} = \int {\rm d}x{\rm d}y\hat{\psi}^\dagger[-{\rm i}\lambda_{\rm SO}(\kappa_x\partial_y\hat{\sigma}_x - \kappa_y\partial_x\hat{\sigma}_y)]\hat{\psi}$ with $\hat{\sigma}_{x,y}$ being the Pauli matrices, κ_x and κ_y denote the strengths of SOC in the x- and y-directions, respectively. Note also that, the SO coupling terms are usually classified as ones of the Rashba and Dresselhaus types, or mixtures of both. In the present work, we consider the Rashba type SO coupling. So far, the configuration of SO coupling realized experimentally is a special one as an equal weight combination of Rashba-type and Dresselhaus-type SO couplings. Thus it is effective just in one dimension.[7] Although we choose a Rashba-type SOC, our conclusions are equally valid for the Dresselhaus-type one.

The assumption of a very strong confinement along the z axis, i.e., $\hbar\omega_z$ being much larger than any other energy scale in the problem is assumed, which allows us to treat the problem as quasi-two-dimensional (2D). In this work, the external potential in the following shape is assumed to be equal to these two components

$$V(r) = \min\left\{\frac{1}{2}m\omega_0^2(r_\perp - R_0)^2, \frac{1}{2}m\omega_1^2(r_\perp - R_1)^2\right\} + \frac{1}{2}m\omega_z z^2. \tag{2}$$

Here, $r_\perp = (x,y)$ is the position vector on the x–y plane. The two parabola in $V(r)$ with frequencies ω_0 and ω_1 (here we set $\omega = \omega_0/4$ and $\omega_1/\omega_0 = 5/4$ to make the product of the "width" of each annulus times the radius of each annulus to be comparable to each other) are centered at the positions $r_\perp = R_0 = 2a_0$ and $r_\perp = R_1 = 4a_0$ with $a_0 = [\hbar/(m\omega)]^{1/2}$ being the oscillator length.[37–39] Under these conditions, $V(r_\perp)$ describes a concentrically coupled annular trap, as shown in Fig. 1.

To obtain the ground state solutions of such a system, it is particularly important to write down the Gross–Pitaevskii energy function of the system, which under the mean-field approximation can be given by

$$\begin{aligned}
&E[\phi_\uparrow, \phi_\downarrow] \\
&= \int {\rm d}x{\rm d}y\Big\{\frac{\hbar\lambda_{\rm R}}{m}[\phi_\uparrow^*(-{\rm i}\kappa_x\partial_y + \kappa_y\partial_x)\phi_\downarrow \\
&\quad + \phi_\downarrow^*(-{\rm i}\kappa_x\partial_y - \kappa_y\partial_x)\phi_\uparrow] \\
&\quad + \phi_\uparrow^*\Big(-\frac{\hbar^2}{2m}\nabla^2 + V(r)\Big)\phi_\uparrow + \phi_\downarrow^*\Big(-\frac{\hbar^2}{2m}\nabla^2 + V(r)\Big)\phi_\downarrow \\
&\quad + \frac{c_0}{2}(|\phi_\uparrow|^2 + |\phi_\downarrow|^2)^2 + \frac{c_2}{2}(|\phi_\uparrow|^2 - |\phi_\downarrow|^2)^2 \\
&\quad + {\rm i}\hbar\Omega\phi_\uparrow^*\Big[x\frac{\partial}{\partial y} - y\frac{\partial}{\partial x}\Big]\phi_\uparrow + {\rm i}\hbar\Omega\phi_\downarrow^*\Big[x\frac{\partial}{\partial y} - y\frac{\partial}{\partial x}\Big]\phi_\downarrow\Big\}.
\end{aligned} \tag{3}$$

The ground state solutions can be obtained by minimizing the GP energy Eq. (3). In the numerical simulations, we employ the normalized gradient flow with backward Euler and second-order centered finite difference discretization within an imaginary-time propagation approach.[40,41] The propagation continues until the fluctuation in the norm of the wave function becomes smaller than 10^{-6}. One should keep in mind that all the parameters used in the following numerical simulations are all dimensionless. For the contact interaction, it is scaled by $\hbar\omega a_0^2 = \hbar^2/m$; while $\tilde{\lambda}_{\rm so} = a_0/a_\lambda = (m/h^3)^{1/2}\lambda_{\rm R}/\omega^{1/2}$ for the SO coupling with $a_\lambda = \hbar^2/(m\lambda_{\rm R})$.

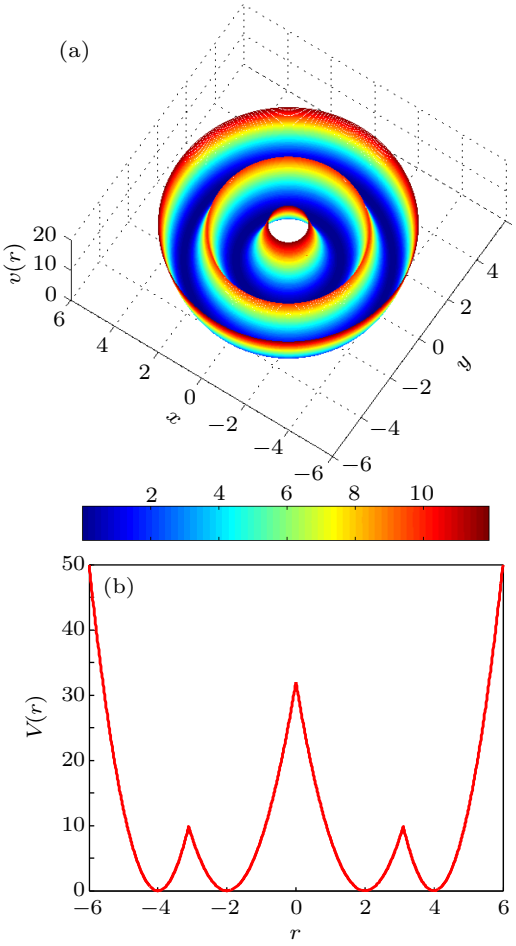


Fig. 1. (color online) (a) Schematic illustration of the concentrically coupled annular trap. (b) The corresponding one-dimensional plot of the external potential. Here, $\omega = \omega_0/4$, $\omega_1/\omega_0 = 5/4$, $R_0 = 2a_0$, and $R_1 = 4a_0$ with $a_0 = [\hbar/(m\omega)]^{1/2}$ being the oscillator length.

3. Numerical results and discussion

Now we perform a detailed numerical study of the combined effects of anisotropic spin–orbit coupling and rotation

on the ground state properties of the system under consideration. In the absence of SOC and rotation, three different phases: (i) coexistence of the two components, (ii) azimuthal separation, and (iii) radial separation are identified through varying the intra-component interaction.[39] Following this line, we also select three typical sets of parameters for the contact interaction: (i) $g_{12} = 55$ and $g = 5$, (ii) $g_{12} = 55$ and $g = 15$, and (iii) $g_{12} = 55$ and $g = 60$, to find out the combined effects of anisotropic SO coupling and rotation. Meanwhile, we define the overlap between the two condensate wave functions to distinguish phase separation and phase mixing. In what follows, we will find that these overlaps are close to 0 and 1, corresponding to phase separation and phase mixing, respectively.[42,43]

We first investigate the ground state of the system for fixed contact interactions $g_{12} = 55$ and $g = 5$. In the absence of SOC and rotation, the system is in azimuthal phase separation, as shown in the upper left corner of Fig. 2, which shows the typical density profiles of a pseudo spin-1/2 SO coupled condensate for variable SOC and rotation. For each fixed rotational frequency, the strength of SO coupling in the x-axis direction, κ_x, is increased from zero up to 1; while κ_y is set to zero. Shown in the first row of Fig. 2 is the numerical result for the limiting case without rotation, where a phase transition from azimuthal phase separation to phase coexistence occurs with the strength of SOC increasing. On the contrary, if an isotropic SOC ($\kappa_x = \kappa_y \neq 0$) is considered, no phase transition occurs. In the latter case, some high energy atoms are repelled to the outer ring and form an alternative arrangement of the two components, hence the system remains in the azimuthal phase separation.[34] Typical example of such phase transition is shown in Figs. 2(b)–2(d) of the first row.

In the opposite limit of $\kappa_x = 0$, the rotation can be absorbed by a change of the reference frame. In this case, the atoms feel an outward centrifugal force due to the presence of a centrifugal potential as $-m\Omega^2(x^2+y^2)/2$. Thus more high energy atoms are repelled to the outer ring and form an alternative arrangement of the two components, as shown in the left column of Fig. 2. Actually, this observation also holds for the left column of Fig. 3. When both the SOC and rotation are taken into account, again we find a similar result to our previous work.[35] That is, the rotation determines the location of an atom without changing the type of ground state phase, and the system eventually develops to phase coexistence with further increasing the SOC and rotational frequency.

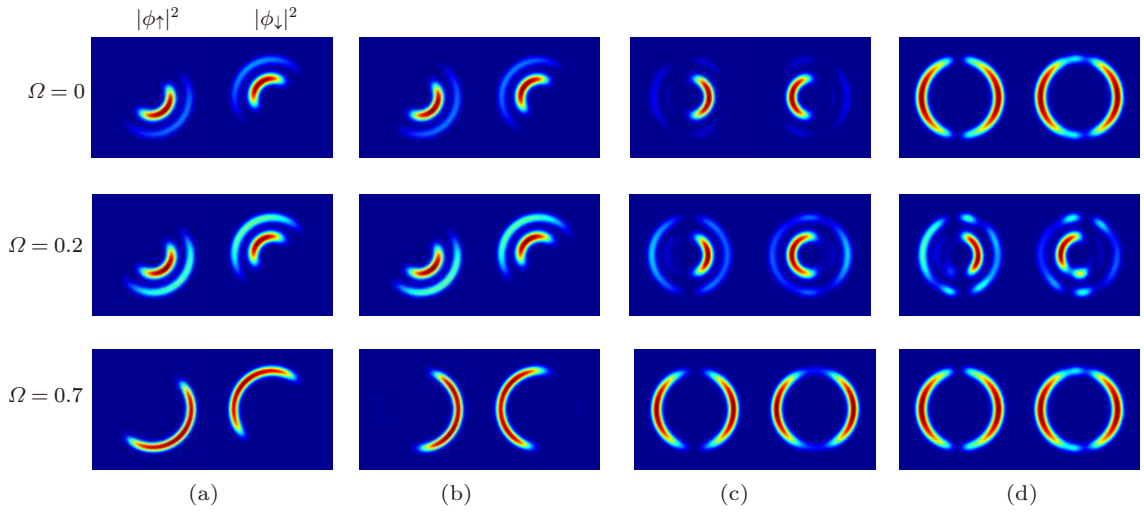


Fig. 2. (color online) Typical density profiles of a pseudo spin-1/2 SO coupled condensate for contact interactions $g_{12} = 55$ and $g = 5$, and for the rotational frequency $\Omega = 0, 0.2, 0.7$, corresponding to the first to third rows, respectively. Note that for each row, the strength of spin–orbit coupling $\kappa_y = 0$ and $\kappa_x = 0, 0.2, 0.7, 1$, corresponds to panels (a)–(d), respectively.

Figure 3 shows the typical density profiles of the system for fixed contact interactions $g_{12} = 55$ and $g = 15$, where the system is in radial phase separation in the absence of SO coupling and rotation. Another interesting observation is that, in the absence of rotation, if and only if an anisotropic SOC with $\kappa_y = 0$ is considered, the system can eventually develop to the azimuthal phase separation. It is obviously different from our previous results, where the system undergoes a phase transition from radial to azimuthal phase separation, but eventually returns to the initially radial phase separation.[34] Similar to our previous case, the system again develops to the phase coexistence phase with increasing both the SO coupling and rotation, as shown in the lower right of Fig. 3.

Note also that, our results are to some extent similar to the previous results obtained by Merhasin *et al.*, where linear coupling (without spatial derivatives) also induced a mixing transition.[42] In that study, the stationary solutions are also obtained numerically by the well-known method of the imaginary-time integration. Hence we conclude that besides the s-wave interactions, both the SOC and the linear coupling can be used to obtain the desired ground state phases.

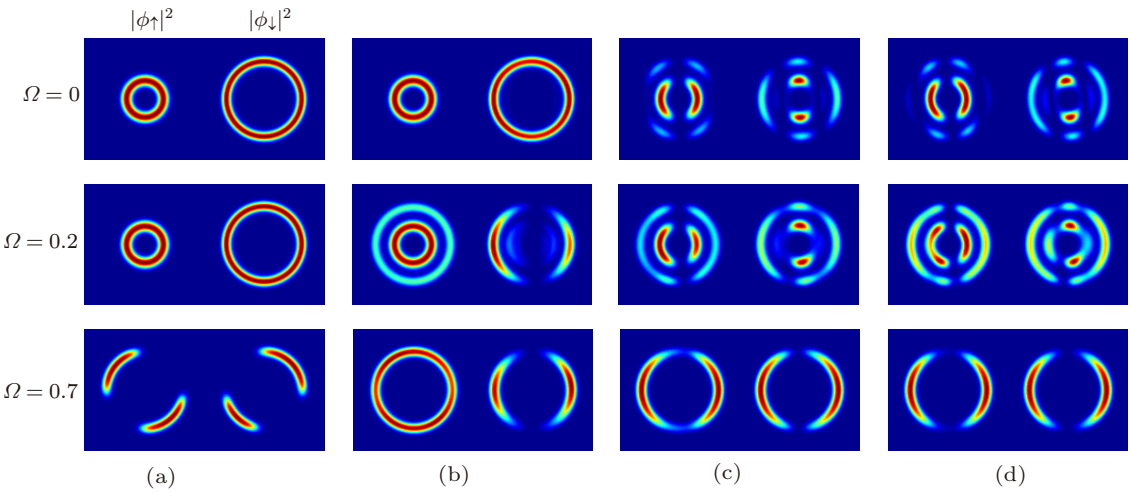


Fig. 3. (color online) Typical density profiles of a pseudo spin-1/2 SO coupled condensate for contact interactions $g_{12} = 55$ and $g = 15$, and for the rotational frequency $\Omega = 0, 0.2, 0.7$, corresponding to the first to third rows, respectively. Note that for each row, the strength of spin–orbit coupling $\kappa_y = 0$ and $\kappa_x = 0, 0.2, 0.7, 1$, corresponds to panels (a)–(d), respectively.

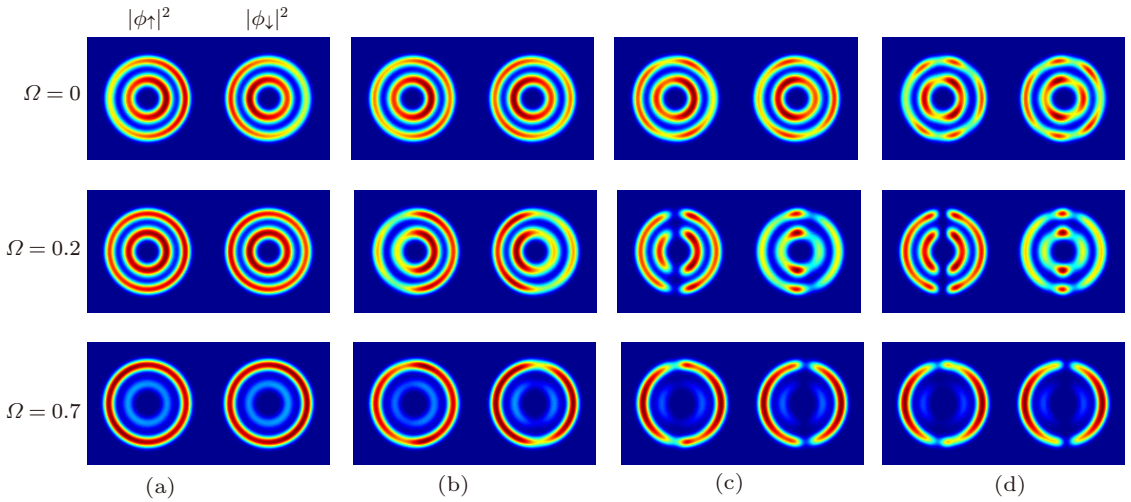


Fig. 4. (color online) Typical density profiles of a pseudo spin-1/2 SO coupled condensate for contact interactions $g_{12} = 55$ and $g = 60$, and for the rotational frequency $\Omega = 0, 0.2, 0.7$, corresponding to the first to third rows, respectively. Note that for each row, κ_y is fixed to 1 and $\kappa_x = 0, 0.2, 0.7, 1$, corresponding to panels (a)–(d), respectively.

Finally, we discuss the situation where the system is initially in phase coexistence for fixed contact interaction $g_{12} = 55$ and $g = 60$. With the same procedure as before, our results show that the system is always in phase coexistence no matter the SOC and rotation are opened respectively or jointly. In our previous work,[34] where an isotropic SO coupling is taken into account, phase transition between phase coexistence and azimuthal phase separation occurs. However, for our system, if the SO coupling is only in the y axis, no phase transition occurs, as shown in the first column of Fig. 4.

Last but not least, we would like to note that while we have chosen the above particular parameter sets, we also have conducted extensive numerical simulations over a range of different parameter sets, and find that the parameter sets used in this work illustrate well the possible ground states and their phase transitions. As concerns the physical parameters adopted in the numerical simulations, we choose the pseudo-spin-1/2 BEC of ^{87}Rb with atomic mass $m = 1.4442 \times 10^{-25}$ Kg, which can be realized by selecting two internal "spin" states from a spin-1 Bose gas of ^{87}Rb atoms with the F = 1 ground electronic manifold. The interactions between atoms can be controlled by means of the Feshbach resonance, which makes it possible to change the scattering lengths for collisions between atoms in the BEC by dint of an external magnetic field, or properly tuned optical signal.[42] Moreover, the strength of the SO coupling can be precisely controlled by optics means-from no coupling at all to strong coupling, which scales with the laser's intensity.

4. Conclusion

To summarize, we have investigated the ground state properties of a pseudo spin-1/2 SO coupled condensate confined in concentrically coupled annular potential for fixed contact interactions. The ground state solutions are studied as a function of the anisotropic SO coupling, as well as the rota-

tion, showing a rich ground state structure. Compared with the isotropic SOC, the anisotropic one can be used to induce more different phase transitions among azimuthal and radial phase separation, and phase mixing. Since these different ground state phases can be described starting from a simple theoretical framework, and the phase transition can be readily manipulated in real experiments, our results promise to shed insight on the topic of orbital physics in ultracold quantum gases.

References

[1] Xiao D, Chang M C and Niu Q 2010 *Rev. Mod. Phys.* **82** 1959
[2] Hasan M Z and Kane C L 2010 *Rev. Mod. Phys.* **82** 3045
[3] Qi X L and Zhang S C 2010 *Phys. Today* **63** 33
[4] Zhang Y P, Mao L and Zhang C W 2012 *Phys. Rev. Lett.* **108** 035302
[5] Lin Y J, Compton R L, Jimnez-Garca K, Porto J V and Spielman I B 2009 *Nature* **462** 628
[6] Lin Y J, Compton R L, Perry A R, Phillips W D, Porto J V and Spielman I B 2009 *Phys. Rev. Lett.* **102** 130401
[7] Lin Y J, Jiménez-García K and Spielman I B 2011 *Nature* **471** 83
[8] Osterloh K, Baig M, Santos L, Zoller P and Lewenstein M 2005 *Phys. Rev. Lett.* **95** 010403
[9] Stanescu T D, Zhang C and Galitski V 2007 *Phys. Rev. Lett.* **99** 110403
[10] Campbell D L, Juzeliunas G and Spielman I B 2011 *Phys. Rev. A* **84** 025602
[11] Chapman M and Sá de Melo C 2011 *Nature* **471** 41
[12] Zhang X F, Zhang P, He W Q and Liu X X 2011 *Chin. Phys. B* **20** 020307
[13] Li Z D, Yao S F and Li Q Y 2011 *Chin. Phys. B* **20** 110307
[14] Wu C J, Ian M S and Zhou X F 2011 *Chin. Phys. Lett.* **28** 097102
[15] Wu C and Zhang S C 2004 *Phys. Rev. Lett.* **93** 036403
[16] Wang C, Gao C, Jian C M and Zhai H 2010 *Phys. Rev. Lett.* **105** 160403
[17] Xu X Q and Han J H 2011 *Phys. Rev. Lett.* **107** 200401
[18] Ho T L and Zhang S 2011 *Phys. Rev. Lett.* **107** 150403
[19] Sinha S, Nath R and Santos L 2011 *Phys. Rev. Lett.* **107** 270401
[20] Kawakami T, Mizushima T, Nitta M and Machida K 2012 *Phys. Rev. Lett.* **109** 015301
[21] Liao R, Yu Y X and Liu W M 2012 *Phys. Rev. Lett.* **108** 080406
[22] Deng Y, Cheng J, Jing H, Sun C P and Yi S 2012 *Phys. Rev. Lett.* **108** 125301
[23] Hu H, Ramachandhran B, Pu H and Liu X J 2012 *Phys. Rev. Lett.* **108** 010402
[24] Zhou X F, Zhou J and Wu C 2011 *Phys. Rev. A* **84** 063624
[25] Radić J, Sedrakyan T A, Spielman I B and Galitski V 2011 *Phys. Rev. A* **84** 063604
[26] Xu Z F, Lü R and You L 2011 *Phys. Rev. A* **83** 053602
[27] Su S W, Liu I K, Tsai Y C, Liu W M and Gou S C 2012 *Phys. Rev. A* **86** 023601
[28] Wen L, Sun Q, Wang H Q, Ji A C and Liu W M 2012 *Phys. Rev. A* **86** 043602
[29] Hu H and Liu X J 2012 *Phys. Rev. A* **85** 013619
[30] Ozawa T and Baym G 2012 *Phys. Rev. A* **85** 063623
[31] Zhou L, Pu H and Zhang W P 2013 *Phys. Rev. A* **87** 023625
[32] Salasnich L and Malomed B A 2013 *Phys. Rev. A* **87** 063625
[33] Zezyulin D A, Driben R, Konotop V V and Malomed B A 2013 *Phys. Rev. A* **88** 013607
[34] Zhang X F, Dong R F, Liu T, Liu W M and Zhang S G 2012 *Phys. Rev. A* **86** 063628
[35] Zhang X F, Gao R S, Wang X, Dong R F, Liu T and Zhang S G 2013 *Phys. Lett. A* **377** 1109
[36] Zhang X F, Li B and Zhang S G 2013 *Laser Phys.* **23** 105501
[37] Brand J, Haigh T J and Zülicke U 2009 *Phys. Rev. A* **80** 011602
[38] Smyrnakis J, Bargi S, Kavoulakis G M, Magiropoulos M, Kärkkäinen K and Reimann S M 2009 *Phys. Rev. Lett.* **103** 100404
[39] Malet F, Kavoulakis G M and Reimann S M 2010 *Phys. Rev. A* **81** 013630
[40] Bao W Z and Tang W J 2003 *J. Comput. Phys.* **187** 230
[41] Bao W Z and Shen J 2004 *SIAM J. Sci. Comput.* **25** 1674
[42] Merhasin I, Malomed B A and Driben R 2005 *J. Phys. B* **38** 877
[43] Wen L, Liu W M, Cai Y, Zhang J M and Hu J 2012 *Phys. Rev. A* **85** 043602